Eigen Spreading

Feb 27, 2008

Sponsored by

Defense Advanced Research projects Agency (DOD)

Advanced Technology Office

ARPA Order Nr. U708-43

Issued by the U.S. Army Aviation and Missile Command Under Contract No. W31P4Q-05-C-0272

Name of Contractor: **Silvus Technologies, Inc.**
(Formerly Silvus Communication Systems, Inc)

Project Scientist: **Weijun Zhu, Babak Daneshrad**
Business Address: **10990 Wilshire Blvd., Suite 440**
LA, CA 90024

Phone Number: **(310) 479-3333**

Effective Date: **Aug. 18, 2005**
Short Title of Work: **Eigen Spreading**

Contract Expiration Date: **03/31/08**
Reporting Period: **12/1/07 – 12/31/07**

Disclaimer

UNCLASSIFIED

1. Introduction

In this contract we investigated the potential of using multiple antennas to improve communications in an interference/jammer intensive environment. The motivation for the work and the deviation from traditional beam forming and beam nulling techniques comes from the recent advances in the field of multi input multi output (MIMO) wireless communications which was fuelled by the seminal work of Foschini, Gans and Teletar over a decade ago. MIMO techniques have shown tremendous improvement in the throughput and quality of wireless data communication links in commercial and interference limited scenarios, however, their utility to improve interference and jammer immunity has hitherto been unexplored.

MIMO techniques augment the traditional 2 dimensional signalling space that consist of time and frequency into a three dimensional space consisting of time, frequency, and space. The spatial element of the channel is energized via the use of multiple, spatially separate antennas. Commercial systems exploit the third signalling dimension to achieve diversity and/or spatial multiplexing gain, however, we want to see if it is possible to exploit it to achieve improved LPD and AJ immunity.

To deliver a waveform that is inherently jam resistant and immune to detection and interception, the properties of the environment must be factored into the transmission. This means that the waveform itself must be cognisant of the geography and geometry of the environment. MIMO techniques do exactly that [1][2][3]. They transmit parallel sets of data along the Eigenvectors of the channel matrix, which in turn is a function of the unique environmental geometry that exists between the transmitter and receiver. These Eigenvectors will be different once the geographical location of the transmitter, the receiver or the interference source changes.

In this work we exploit the environmentally unique channels inherent in MIMO communications to deliver a new spread spectrum strategy that is more spatially focused than traditional DSSS (direct sequence spread spectrum) and FHSS (frequency hopped spread spectrum) techniques. However, the proposed technique must be complementary to DSSS and FHSS systems.

Our initial strategy was to exploit the notion of spatial, or eigen spreading and in so doing achieve additional processing gain. Investigation of this approach showed an additional 6 to 7 dB of processing gain that could complement DSSS processing gain. We then investigated the utility of eigen beamnulling to improve the AJ properties of the received signal. The proposed method showed in excess of 20 dB of jammer mitigation in multipath rich Rayleigh flat fading environments. To accommodate the various types of processing and to deliver a scalable end solution we investigated an architecture for a general purpose MIMO engine that could handle the types of processing needed for traditional mimo based communications such as spatial multiplexing and space time coding, along with the requirements for eigen-spreading and eigen beamnulling. Finally we developed an RF transceiver module for the SDR radios developed under other programs to enable eigen spreading and beamnulling.

To support this effort, a few parallel tasks took place: the algorithm development, the hardware description language (HDL) code development, software development on hardware interface and human interface sides, and hardware development. For the algorithm development, the focus was on the multi-antenna algorithms and all the sub engines needed for its support. In the HDL code development, not only the algorithms were ported but also other code needed such as an packet interface/parser for the entire system to operate. The control and data harvesting was performed using a PC and C language code was also developed. The two basic parts of these C codes were to support communication with the radio through the LMAC and human interface code to interact with the user. The major hardware effort in this contract was to build a new RF board.

2. MIMO Overview

Multi-Antenna Processing

Since the seminal work of Foschini and Gans which revolutionized wireless data communications, multi antenna processing has been shown to have tremendous impact on the overall performance of a wireless link. There are a multiplicity of multi antenna techniques each suited for a given range of applications, missions, and environments. These include: beamforming, diversity, space-time coding, eigen beamforming, and spatial multiplexing. There is no one antenna technique that is best for all scenarios, rather each is suited for a particular mission and environmental conditions. To deliver optimal connectivity, a radio must be able to effortlessly move between these modes.

Traditional Beamforming (also referred to as phased array beamforming) refers to the use of multiple omini directional antennas to create a directional antenna and thus achieve directivity and antenna gain. This type of antenna processing is ideal in wide plains and other environments where there are no local scattering elements in the vicinity of array, and the channel can be modelled as an AWGN (additive white Gaussian noise channel).

Diversity Processing is ideal for communications in Rayleigh flat fading channel conditions which are typical of environments with many multipath reflections. In this situation the reflections cause different copies of the signal to arrive at the receiver with different phases. Sometimes the phase difference can be 180 degrees which will cause a deep fade in the received signal strength. The impact of Rayleigh flat fading on the bit error rate performance of a communication system can be drastic. Figure 1 was obtained from **Error! Reference source not found.**and shows that a QPSK system operating in an AWGN channel can achieve a BER of 10^{-6} (such BERs are representative of the quality needed for good HD video transmission) with 10 dB

SNR. However, achieving the same BER in a Rayleigh fading channel requires close to 53 dB in SNR. Applying fourth order maximum ratio combining diversity to the link will reduce the SNR requirement by 40 dB to approximately 13 dB, as shown in Figure 1. Assuming a realistic path loss exponent of 3 (a path loss exponent of 2 is only valid in free space and is overly optimistic), the 40 dB improvement in link budget translates into a 21x increase in range, or a 464x increase in the coverage area relative to a single antenna system. This suggests that a system with diversity processing will be much more adept at maintaining communications in urban environments.

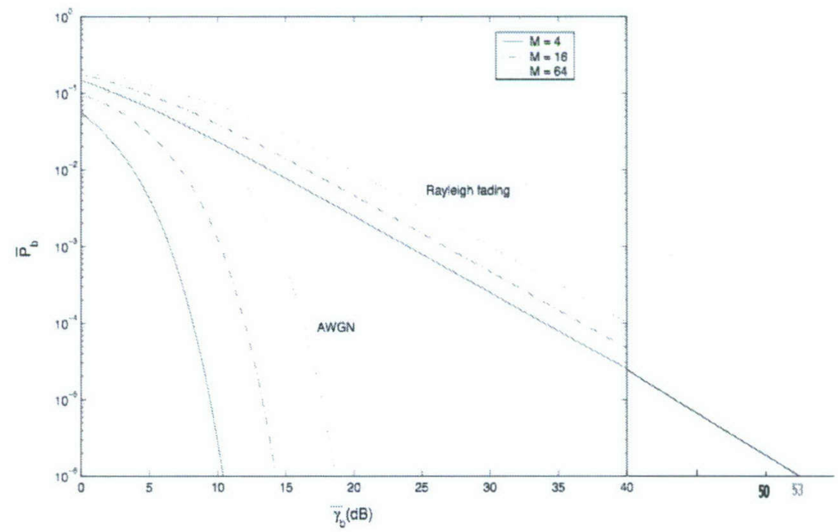

Figure 1, BER in Rayleigh fading channel w/ 53 dB in SNR [14, p. 186].

Eigen Beamforming is analogous in nature to beamforming but is meant for scatter rich environments, and does not need optimum antenna placement. In fact, the eigen-beamforming algorithms will default to the traditional beamforming algorithms in free space or in open fields.

Space-Time Coding is a very powerful diversity technique that allows a system to achieve diversity on the transmit side. Whereas traditional diversity techniques use one transmit (TX) antenna and *M* receive (RX) antennas. With space-time coding one can achieve the same diversity gain with *M* TX antennas and one RX antenna. In our proposed system where each end of the link can have as many as 4 antennas STC will be used to increase the diversity order to a maximum of 8. Referring back to Figure 2link budget improvement of 45.5 dB can be achieved in this case.

Spatial Multiplexing is the most advanced of all multi antenna based algorithms. It is based on the pioneering work of Bell Labs Researchers and has revolutionized the commercial wireless communications industry. Spatial Multiplexing is a means of increasing throughput without increasing bandwidth. It uses a three dimensional signalling scheme consisting of time, frequency and space, as compared to the traditional 2D signalling space consisting of time and frequency. SM thrives on multipath and provides a linear increase in the capacity of a wireless link compared to a logarithmic improvement delivered by phased array beamforming techniques used in the past. Figure 2 shows this capacity trend.

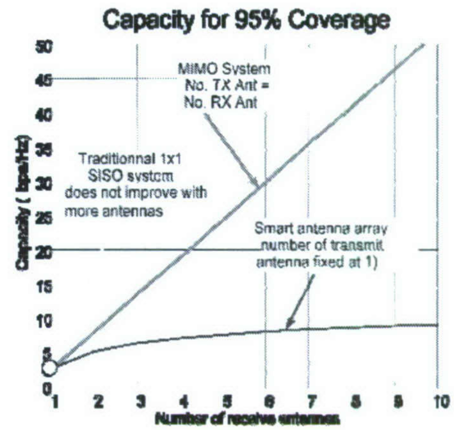

Figure 2, Spatial Multiplexing gains.

Spatial Multiplexing can also help reduce the total transmit power, as it allows a system to deliver the same throughput with less SNR. This is depicted in Table 1.

How it works

A MIMO wireless system consists of *N* transmit antennas and *M* receive antennas. However, unlike phased array systems where a single information stream x(t), is transmitted on all transmitters and then received at the receiver antennas, MIMO systems transmit different information streams x(t), y(t), z(t), on each transmit antenna. These are independent information streams being sent simultaneously and in the same frequency band. At first glance one might say that the transmitted signals interfere with one another. In reality, however, the signal arriving at each receiver antenna will be a linear combination of the *N* transmitted signals. Figure 3 shows a MIMO system with three transmit and three receive antennas. The received signals $r_1(t)$, $r_2(t)$, $r_3(t)$ at each of the three received antennas are a linear combinations of x(t), y(t), z(t). The coefficients $\{a_{ij}\}$ represent the channel weights corresponding to the attenuation seen between each transmit-receive antenna pair. The affect is that we have a system of three equations and three unknowns as shown below.

MIMO Config.	95 % Capacity at 20 dB SNR	Required SNR for 1 bps/Hz of capacity
1x1	2.6 bits/sec/Hz	12.8 dB
2x2	8.0 bits/sec/Hz	1.2 dB
4x4	19.0 bits/sec/Hz	-4.9 dB
8x8	40.8 bits/sec/Hz	-9.3 dB

Table 1, Spatial Multiplexing TX power reduction gains.

$$\bar{r} = \bar{A}\begin{bmatrix} x \\ y \\ z \end{bmatrix} \qquad \begin{aligned} r_1(t) &= a_{11}x(t) + a_{12}y(t) + a_{13}z(t) \\ r_2(t) &= a_{21}x(t) + a_{22}y(t) + a_{23}z(t) \\ r_3(t) &= a_{31}x(t) + a_{32}y(t) + a_{33}z(t) \end{aligned}$$

In general the matrix, A, of channel coefficients $\{a_{ij}\}$ must be invertible for MIMO systems to live up to their promise. It has been proven that the likelihood for A to be invertible increases as the number of multipaths and reflections in the vicinity of the transmitter or receiver increases. The impact of this is that in a Rayleigh fading environment with spatial independence, there are essentially *NM* levels of diversity available and there are *min(N,M)* independent parallel channels that could be established. Increase in the diversity order results in significant reduction of the total transmit power for the same level of performance. On the other hand, increases in the number of parallel channels translates into an increase in the achievable data rate within the same bandwidth.

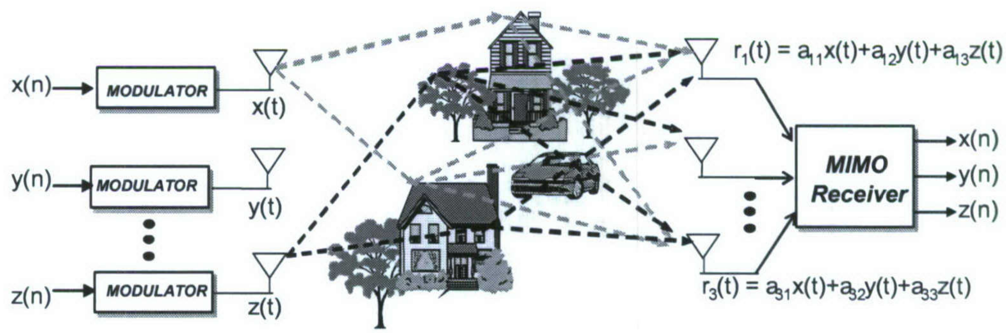

Figure 3, MIMO transmission and reception in a dispersive environment. In MIMO systems different information is transmitted simultaneously on each transmit antenna.

3. Eigen Spreading

The notion of eigen spreading that we explored as part of the proposed work exploited the matrix structure of the wireless MIMO channel coupled with the use of OFDM in wideband dispersive conditions. This approach initially showed promise for the improvement of AJ/LPD/LPI characteristics of a waveform. To illustrate, let us consider an 8x8 wireless communication system. In this case each OFDM subcarrier will have eight spatial eigen modes associated with it. In much the same fashion as in DSSS, the transmitter and receiver will distribute the bit energy randomly among all subcarriers as well as each eigen mode within a subcarrier.

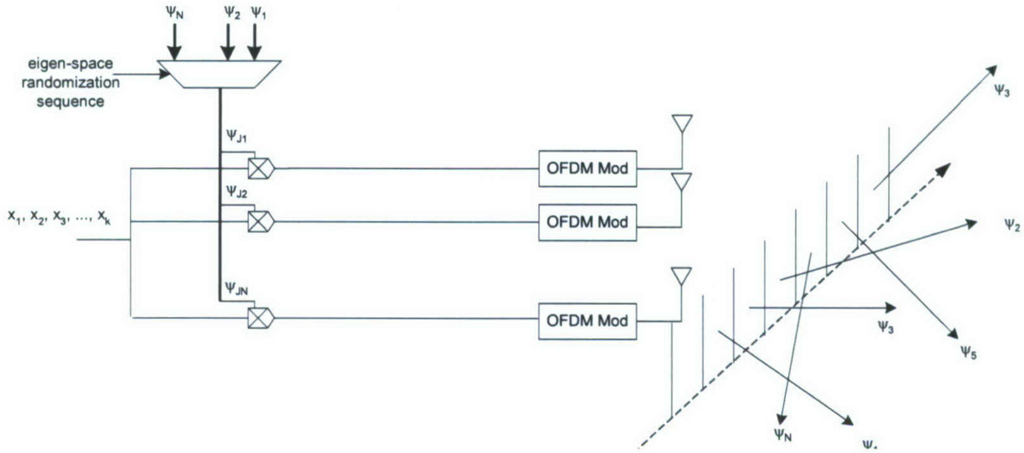

Figure 4, Top level block diagram of the MIMO-OFDM eigen spreading concept.

This Eigen concept is clarified in Figure 4. In the proposed system the transmitter unit scrambles the data using the spatial properties of the communication channel ***H***. Only a unit which has knowledge of the MIMO communication channel ***H*** is able to correctly decipher the message. Furthermore, the transmitter will maximize the power transmitted along the channel ***H*** and minimize the power transmitted in other directions. This same mechanism reduces the probability of an enemy unit detecting the transmission. The receiver unit also uses MIMO technology to correctly receive and descramble the transmitted signal and performs spatial interference cancellation to provide a high degree of immunity to jammer interference. The system shown, in Figure 4, assumes that the underlying modulation scheme is OFDM (orthogonal frequency division multiplexing) [3]. OFDM provides a mechanism by which a broadband signal is subdivided into many smaller subcarriers that are placed arbitrarily close to one another in the frequency domain. The proposed eigen-spreading technique takes advantage of this by allowing each individual sub-carrier of the OFDM modulated waveform to be transmitted in the direction of one of the *N* randomly chosen Eigen-vectors within the Eigen-space. Figure 5 shows the top level block diagram of a generic MIMO OFDM system.

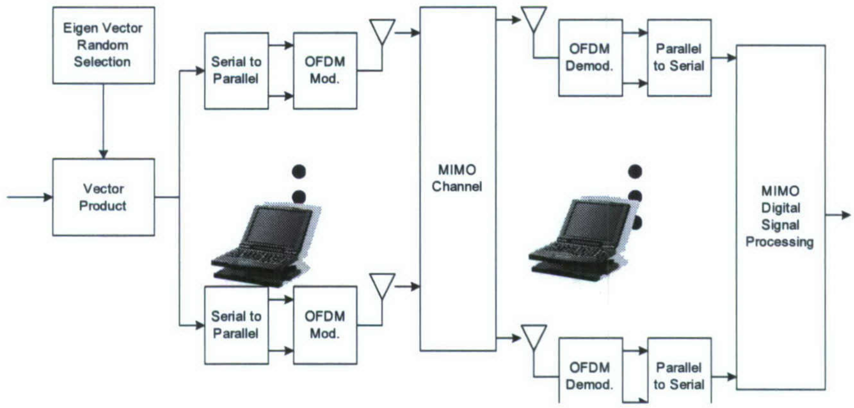

Figure 5, Top level block diagram of a MIMO OFDM system

In the proposed architecture, the transmitter determines the Eigen vector of the MIMO transmission channel $\boldsymbol{H}$. The knowledge of $\boldsymbol{H}$ at the transmitter can be obtained by using the channel reciprocity of a Time Division Duplex (TDD) system or by feedback from the receiver. For each transmitted symbol, the transmitter randomly chooses one of the Eigen vectors for transmission. At the receiver, OFDM demodulation is first used to recover the transmitted data on the sub-carriers. After parallel to serial conversion of the OFDM sub-carriers, the data is presented to the MIMO digital signal processing unit to recover the transmitted data streams. The MIMO signal processing unit provides multiple functionalities. It inverts the channel to recover the data transmitted from the different antennas as well as Eigen vector spatial descrambling.

On the other hand, if anti jamming is the main concern, then the MIMO capability at the transmitter and the receiver can be exploited in a different manner. The best immunity to jamming can be achieved by using a non symmetric configuration whereby the receiver is outfitted with more antennas as compared to the transmitter. Running an MMSE based algorithm at the receiver will automatically utilize the additional degrees of freedom at the receiver to effectively null out the jammer or interferer in the spatial domain. This is different from traditional beam nulling since the structure of the channel matrix is an integral part of the nulling process. In the case where this additional degree of freedom is not available, we will incorporate notions similar to those used in frequency hopped spread spectrum systems. In that we look to randomize the signal along the many eigenvectors at the transmitter and then tune the receiver to the particular eigenvector that is being transmitted on. In this situation, since the enemy jammer location is typically fixed the total jammer energy that enters the receiver will be averaged over the eigenvectors used for reception.

The notion of eigen spreading is a powerful one. In fact studies showed good improvement in the desirable attributes of the signal. However, the overhead in processing and synchronization in such a system could be quite significant and might compromise, from a practical perspective the benefits of the eigen spreading concept.

In the course of the work we defined a metric that measures the ratio of the total energy received at the friendly site to the total energy received at the enemy site. This provides a lower bound on the LPD performance improvement achievable with MIMO techniques. We define the metric that we term the ***covert gain*** (CG) as follows:

$$CG = 10\log\left(\frac{E\left\{\|H\|_F^2\right\}}{E\left\{\|H_e\|_F^2\right\}}\right)$$

Where H is the channel between the transmitter and the receiver, and $\boldsymbol{H_e}$ is the channel between the transmitter and the enemy. The operator $\|\bullet\|_F^2$ was defined to be the trace of $\boldsymbol{H^H H}$. Figure 6 shows the plot of the covert gain as a function of the number of transmit and receive antennas assuming that the enemy has only one antenna. In this case, the channel matrix is assumed to be a Rayliegh channel. The results show significant improvement with the addition of antennas up to approximately 10 elements. The gain thereafter is asymptotic, reaching a limit of approximately 25 dB.

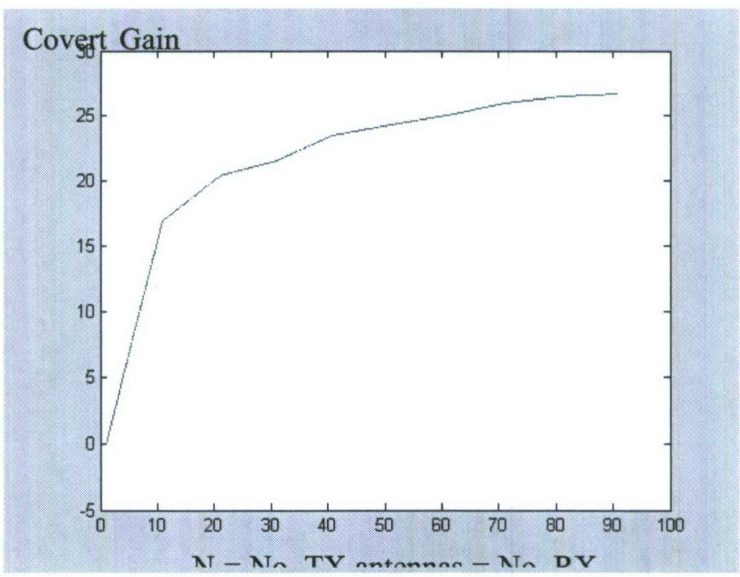

Figure 6, LPD performance as measured by the covert gain, vs. the number of antennas.

4. Universal MIMO Decoder

As part of the work it became clear that a number of different MIMO algorithms must be realized in a given system, moreover, in order to safeguard a system against the threat of becoming obsolete simply because the processing horsepower within a node could not keep up with the ever increasing bandwidth requirements of emerging systems, we investigated a novel architecture for a highly versatile and programmable mimo decoder processing engine. One that could perform singular value decomposition (SVD) along with other operations required for the eigen spreading concept.

Sample use of the MIMO decoder engine

An $N_{tx} \times N_{rx}$ MIMO system with N_{tx} transmitters and N_{rx} receivers can be modeled by:

$$y = Hx + n$$

Where $y_{N_{rx}\times 1}$ is the observation vector, $x_{N_{tx}\times 1}$ is the transmitted vector, and $n_{N_{rx}\times 1}$ is additive Gaussian noise. $H_{N_{rx}\times N_{tx}}$ is the channel matrix, where each element of the matrix is Rayleigh faded. MIMO decoding involves extracting an estimated vector $\hat{x}$ from the observation. This involves an implicit matrix inversion of H or some expression of H.

Methods that perform decoding by performing an explicit (or implicit) matrix inversion, then multiplying this inversion by the observation are classified as linear decoding algorithms. A classical example is MMSE, where the weight matrix minimized the mean square error of the estimate $\hat{x}$:

$$\hat{x} = H^{*}Wy = H^{*}(HH^{*} + \frac{I}{SNR})^{-1} y$$

No assumptions can be made about the structure of the weight matrix W. But by performing a matrix transformation, it can be transformed into a form that can be more easily inverted. One such transformation is QR decomposition. The resultant matrices are both easy to invert: The unitary matrix Q can be inverted by a simple Hermitian operation, and the upper triangular matrix R can be inverted recursively. Not all linear decoding algorithms follow the above steps exactly; the type of decomposition performed may differ. Also the decomposition can be used independently of MMSE. Even if both MMSE and QR decomposition are used, the implementation can be different from the direct method showed above.

Another class of MIMO decoding is maximum likelihood (ML). ML decides on a best guess for $\hat{x}$ by measuring the distance between each candidate vector $\tilde{x}$ and the observation distorted by the channel estimates:

$$\hat{x} = \arg\min\{\| H\tilde{x} - y \|^{2}\}$$

ML is the upper bound of performance (PER). But because the number of candidate vectors $\tilde{x}$ grows quickly with constellation size and number of antennas, straight ML is practical only for smaller systems. For larger systems, sphere decoding (SD) is used to manage the complexity of the problem. SD reduces ML complexity to polynomial at the expense of constant throughput or some performance loss. SD involves performing QR decomposition on the channel matrix. Then by performing a search for a solution using a metric derived from the upper triangular matrix, many potential solutions can be trimmed early.

Most MIMO decoding algorithms can be implemented using a variety of (sometimes substantially different) algorithms. However, a minimum set can be found that covers all algorithms discussed above. All listed algorithms and most of their variants need matrix decomposition, and most use unitary transformations to reach this decomposition [5, 10]. Even sphere decoding uses QR decomposition as a first step in processing channel matrices [12]. All MIMO decoding algorithms also need complex arithmetic matrix/vector processing including: multiplication, division, and addition of matrices, sub-matrices, row/matrix vectors, or any combination of such operands. Table 1 lists the minimum set of common operations needed to support Zero-Forcing (ZF), MMSE, Sphere decoding, and SVD and several variants thereof. The Figure below shows the top level architecture for the mimo decoding engine. The processing section consists of three elements, namely the cordic, the matrix MAC and the divider bank. The cordic section performs the QR decomposition using on the channel Matrix H. The function of the matrix multiply-accumulate (MAC) section is rather self explanatory. It performs vector and matrix based arithmetic operations. Similarly the divider bank is used to realize dedicated divide operation albeit it is used rather infrequently. At the input this block requires the channel estimates, and the demodulated data, and at the output it interfaces with the FEC decoder.

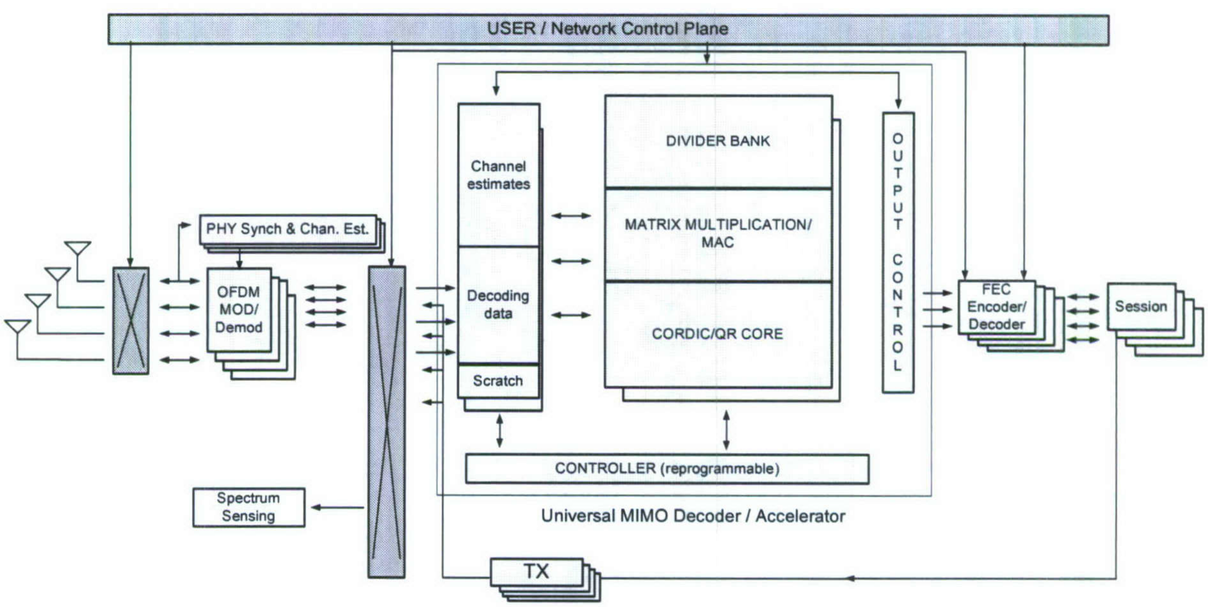

5. Eigen Beamnulling

A subset of the eigen spreading problem was the eigen beamnulling capability at the receiver. This is analogous to traditional beamnulling techniques with the exception that it works well in scatter rich environments. We carried out a series of studies to evaluate the performance of alterantive beam nulling protocols on the overall performance of an OFDM based wireless communication system. The technique that showed a good deal of promise is outlined in the following sections.

5.1. Eigen Nulling

Eigen nulling involves placing a hard null in the direction of the strongest eigenmode. This requires a singular value decomposition of the estimated covariance matrix. The interference mitigation matrix is generated by preserving the weakest left-eigenvalues of the SVD. Since our system is 4x4 we preserved the 3 weakest left-eigenvalues. The eigenvector corresponding to the largest eigenvalue is replaced with the all-zeros vector (Eq. 3). The singular values are assumed to be sorted such that $\sigma_1 > \sigma_2 > \sigma_3 > \sigma_4$.

$$U\Sigma U^* = R \tag{1}$$

$$U\Sigma U^* = \begin{bmatrix} \begin{bmatrix} u_1 \end{bmatrix} & \begin{bmatrix} u_2 \end{bmatrix} & \begin{bmatrix} u_3 \end{bmatrix} & \begin{bmatrix} u_4 \end{bmatrix} \end{bmatrix} \begin{bmatrix} \sigma_1 & & & \\ & \sigma_2 & & \\ & & \sigma_3 & \\ & & & \sigma_4 \end{bmatrix} \begin{bmatrix} \begin{bmatrix} u_1 \end{bmatrix} & \begin{bmatrix} u_2 \end{bmatrix} & \begin{bmatrix} u_3 \end{bmatrix} & \begin{bmatrix} u_4 \end{bmatrix} \end{bmatrix}^* \tag{2}$$

$$W = \begin{bmatrix} \begin{bmatrix} 0 \end{bmatrix} & \begin{bmatrix} u_2 \end{bmatrix} & \begin{bmatrix} u_3 \end{bmatrix} & \begin{bmatrix} u_4 \end{bmatrix} \end{bmatrix}^* \tag{3}$$

This method is effective when the interference power is very high. It places a very harsh null in the direction of the strongest eignenmode. However, as the noise power approaches the noise floor the harshness of the null becomes detrimental to performance. This is because the main lobe of the strongest eigenmode gets distorted by the noise. This also causes the sidelobes to become larger. When the noise power is within 10dB of the interference power the covariance matrix is less likely to optimally identify the interference source with its strongest eigenmode. It is very likely that the eigenmode that gets nulled has been skewed from the optimal value by the noise power. This causes suboptimal nulling and many times hurts the performance. Heuristic schemes can be derived to disable the interference mitigation when the interference power is low, but we will see that there are other methods which offer good performance in low SIR without degrading performance in high SIR.

$$E[yy^*] = E[(Hx + n + \gamma)(Hx + n + \gamma)^*]$$
$$E[yy^*] = HE[xx^*]H^* + R_\gamma + N_0 I$$
$$E[yy^*] = HH^*\|x\|^2 + R_\gamma + N_0 I$$
$$SINR = \frac{HH^*\|x\|^2}{R_\gamma + N_0 I}$$
$$E[y_{clean} y_{clean}^*] = E[(WHx + Wn + W\gamma)(WHx + Wn + W\gamma)^*]$$
$$R_{\gamma+n} = R_\gamma + N_0 I$$
$$R_\gamma = U_\gamma \Sigma_\gamma V_\gamma^* \approx \begin{bmatrix} \begin{bmatrix} u_1 \end{bmatrix} & \begin{bmatrix} u_2 \end{bmatrix} & \begin{bmatrix} u_3 \end{bmatrix} & \begin{bmatrix} u_4 \end{bmatrix} \end{bmatrix} \begin{bmatrix} \sigma_\gamma & & & \\ & \varepsilon & & \\ & & \varepsilon & \\ & & & \varepsilon \end{bmatrix} \begin{bmatrix} [\quad v_1 \quad] \\ [\quad v_2 \quad] \\ [\quad v_3 \quad] \\ [\quad v_4 \quad] \end{bmatrix}^*$$
$$N_0 I = U_n \Sigma_n V_n^* = [I] \begin{bmatrix} \sigma_n & & & \\ & \sigma_n & & \\ & & \sigma_n & \\ & & & \sigma_n \end{bmatrix} [I]$$
$$W^* R_\gamma \approx [0]$$
$$WW^* R_\gamma \approx [0]$$
$$SINR \approx \frac{HH^* WW^* \|x\|^2}{WW^* R_n}$$

5.2. *SINR Gain*

As an initial measure of the performance of these multi-antenna interference mitigation methods we investigated the gain in Signal to Interference+Noise Ratio. This was done by taking the received interference signal and received data signal and applying the interference mitigation matrix to them individually. The signal power and interference power were measured before and after the application of the interference mitigation matrix. The ratio of these powers was averaged over 1000 trials. The SIR was swept from -20dB SIR to +15dB SIR. This was done on channels with varying amounts of delay spread and SNRS of 10dB, 15 dB, 20 dB, and 25dB. The results for eigen-nulling are shown in Figure 7. The results show that nulling can cause a decrease in SIR when the interference power is low, but works reasonably well as the interference power increases.

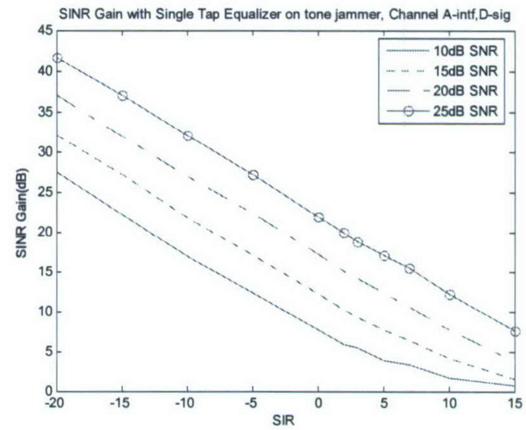

(a)

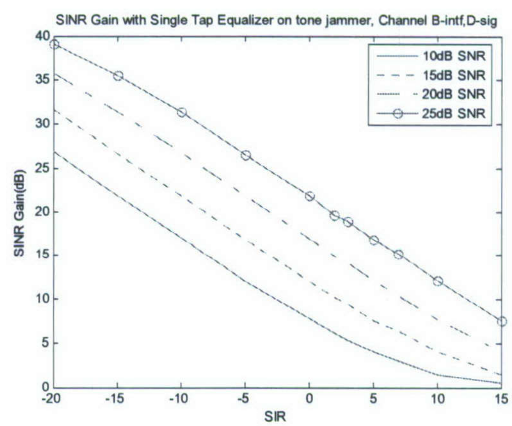

(b)

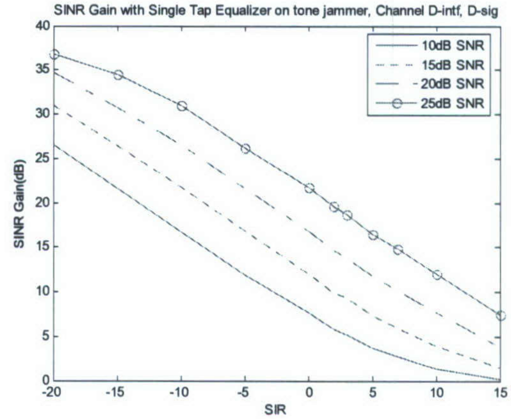

(c)

Figure 7 - SINR Gain for Eigen Nulling

6. LMAC

We started defining the LMAC. The LMAC is an interface between the PHY layer and for example a host PC computer. The PC wants to generate and receive a sequence of data packets. The PC may also want to send/receive control commands such as selecting a rate of transmission or number of antennas used in the MIMO transceiver. Both data and control signals are sent/received from the PC to the LMAC as a sequence of bytes. The LMAC's job is to translate these sequences to a proper timing and formatting that the PHY accepts. We need to define the architecture and definitions for the LMAC.

The LMAC itself is not algorithmically significant, however, from an implementation perspective, the LMAC plays an important role. It provides the ability to carry out first order full duplex communications between the transmitter and receiver so that channel matrix estimates and possible SVD results can be ported back and forth.

During the course of this phase 2 effort the LMAC was fully specified and characterized. The first order VHDL code was written up for the block and simulated, but it was not taken to the FPGA for full operational testing and validation.

7. Hardware Platform

RF subsystem

The RF subsystem (consisting of the four transceiver modules shown in Figure 8), was constructed from various connectorized parts and evaluation boards, in a 4-layer assembly. The main IC of interest is the Maxim MAX2829 RF transceiver. A set of evaluation boards were used to provide an interface for the analog baseband signals to the data converters found on the baseband modules.

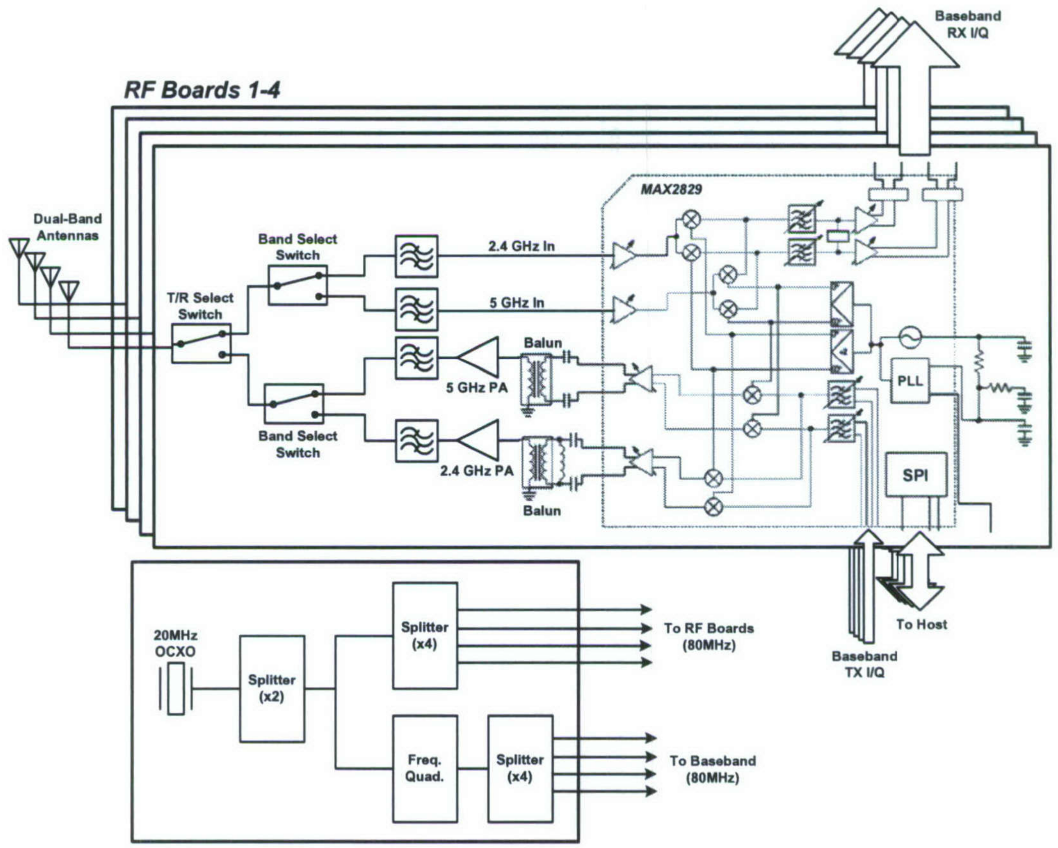

Figure 8. RF Subsystem functional diagram

The RF module for the 4x4 system was developed in parallel with the baseband PHY module. The four transceivers in the RF module are independently configurable through an SPI (serial) interface, controlled via onboard FPGA. Preserving transceiver configuration independence allows a variety of communication schemes such as simultaneously operating in different frequency bands, or even using one transceiver to monitor while the rest maintain an active data channel. Configuration data from the host PC is communicated through the PCI interface on the backplane and then translated and routed to the individual transceivers. The baseband PHY module was married with the RF module via RF cable assemblies and similar RF cables were used to route RF signals to and from the four antennas on the exterior of the chassis.

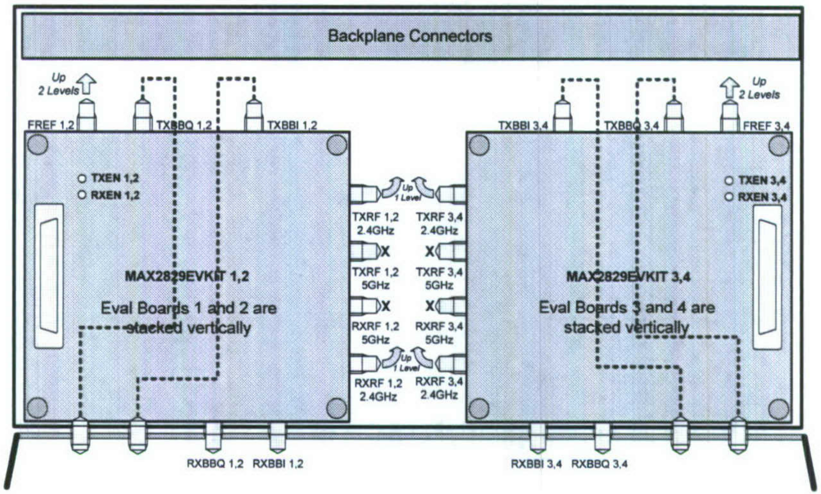

Figure 9. RF Transceiver Layer, cPCI testbed

The four MAX2829 evaluation boards pictured in Figure 9 were stacked vertically, two to a side. Signal cables to the baseband (Tx/Rx) were routed out of the front panel via SMA bulkhead connectors, while signal cables to the power amplifiers (Tx) and bandpass filters (Rx) were routed up to the next layer via a gap in the rear of the metal shielding/mounting plate.

The Rx and Tx connections from the transceiver boards were routed from the lower layer to their respective Maxim MAX2247 power amplifier evaluation boards (Tx) or custom 2.4 GHz bandpass filters. Half-duplexing of the antenna ports was accomplished with RF switches to route signals to and from the external antenna array.

All components were tested individually, including the MAX2829 evaluation boards. Assembly proved to be a challenge. Additionally, mechanical support of the total weight and complex signal routing required some custom drilling and metal work. Upon completion of the testbed RF module assembly, the complete radio testbed system (host PC, baseband module, RF module, antenna array) was verified.

Baseband Subsystem

Our approach to securing the baseband portion of the testbed is quite similar. Given the intense computational requirements of SVD and other matrix mode operations needed to support eigen spreading a combination of high performance FPGAs and DSPs are needed in the digital baseband portion. There are a number of vendors that specialize in providing such systems, chief among them is Pentek, Bittware, and Innovative Integration. The Quixote Board from Innovative Integration in particular seems to be quite promising since it also incorporates the data converter circuitry. Figure 10 shows the block diagram of the Quixote baseband board. Some of the main features of this board are:

- 600 MHz TI TMS320C6416 DSP;

- 200 MHz Virtex II XC2V6000 FPGA (6 Million gates);
- 32 MB on-board shared SDRAM and 8 MB ZBT SBSRAM;
- 2 105 Msamples/s 14 bits ADC and DAC;
- 64/32 bit 66 MHz Compact PCI interface;
- PCI Mezzanine Card (PMC) site with private Jn4 to FPGA;
- Suite of DSP and FPGA development tools.

Having identified the hardware elements of the system, the major task is the portation of the algorithms, and protocols onto the hardware platform for real time operation. This task is probably the major challenge in the development of the testbed. All compute intensive tasks will be implemented on the FPGA with some minor low intensity and decision making tasks assigned to the DSP. Targeting the design to an FPGA will require the development of RTL code, which will then be taken through a synthesis tool followed by final placement and routing on the FPGA. We incorporated a systematic approach for ensuring that the resulting RTL and FPGA code match perfectly and no errors are introduced in the translation process.

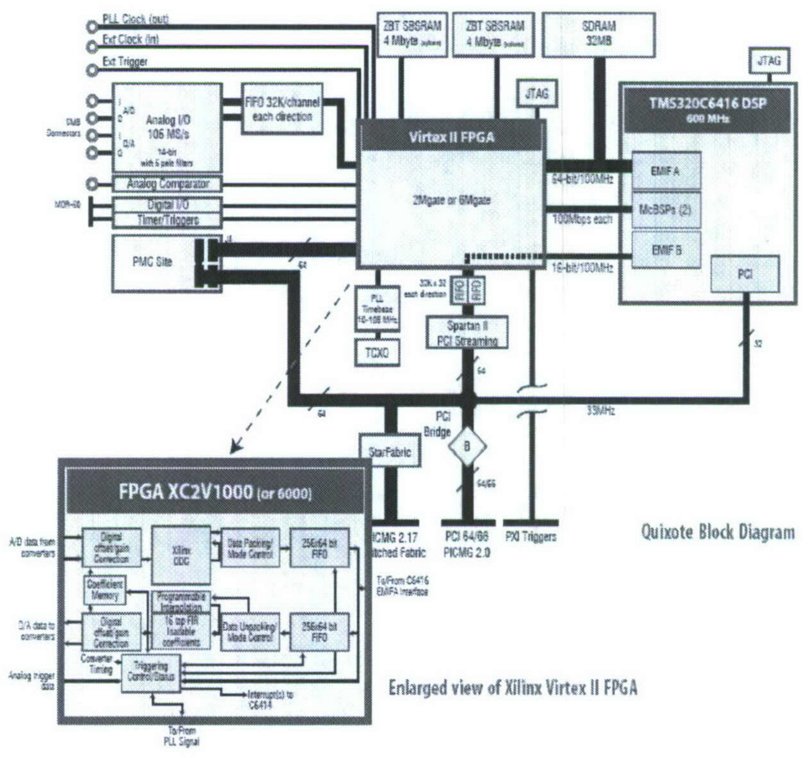

Figure 10, Functional block diagram of Quixote platform

8. References

[1] G. Foschini, and M. Gans, "On Limits of Wireless Communications in a Fading Environment when Using Multiple Antennas," *Wireless Personal Communications*, vol. 6, no.3, pp. 311-335, March 1998.

[2] G. Foschini, "Layered Space-Time Architecture for Wireless Communication in a Fading Environment when Using Multi-Element Antennas," *Bell Labs Technical Journal,* vol. 1, no. 2, pp. 41-59, Fall 1996.

[3] A.J. Paulraj, et. al., "An Overview of MIMO communciations-A Key to Gigabit Wireless," Proceedings of the IEEE, Vol. 92, No. 2, pp. 198 – 218, Feb. 2004.